

Palaeoproterozoic Khondalite Belt in the western North China Craton: New evidence from SHRIMP dating and Hf isotope composition of zircons from metamorphic rocks in the Bayan Ul-Helan Mountains area

DONG ChunYan^{1,2†}, LIU DunYi^{1,2}, LI JunJian³, WAN YuSheng^{1,2}, ZHOU HongYing^{2,3}, LI ChengDong³, YANG YueHeng⁴ & XIE LieWen⁴

¹ Institute of Geology, Chinese Academy of Geological Sciences, Beijing 100037, China;

² Beijing SHRIMP Center, Beijing 100037, China;

³ Tianjin Institute of Geology and Mineral Resources, China Geological Survey, Tianjin 300170, China;

⁴ Institute of Geology and Geophysics, Chinese Academy of Sciences, Beijing 100029, China

Zircon U-Pb age and Hf isotope analyses were made on gneissic granite and garnet-mica two-feldspar gneiss from the Helanshan Group in the Bayan Ul-Helan Mountains area, the western block of the North China Craton (NCC). Zircons from the gneissic granite commonly show core-mantle-rim structures, with magmatic core, metamorphic mantle and rim having ages of 2323 ± 20 Ma, 1923 ± 28 Ma and 1856 ± 12 Ma, respectively. The core, mantle and rim show similar Hf isotope compositions, with single-stage depleted mantle model ages (T_{DM1}) of 2455 to 2655 Ma (19 analyses). Most of the detrital zircons from the garnet-mica two-feldspar paragneiss have a concentrated U-Pb age distribution, with a weighted mean $^{207}\text{Pb}/^{206}\text{Pb}$ age of 1978 ± 17 Ma. A few detrital zircons are older (2871 to 2469 Ma). The age for metamorphic overgrown rim was not determined because of strong Pb loss due to their high U content. The zircons show large variation in Hf isotope composition, with T_{DM1} ages of 1999 to 3047 Ma. In combination with previous studies, the main conclusions are as follows: (1) protolith of the khondalite series in the Helanshan Group formed during Palaeoproterozoic rather than the Archaean as previously considered; (2) The results lend support to the contention that there is a huge Palaeoproterozoic Khondalite (metasedimentary) Belt between the Yinshan Mountains Block and the Ordos Block in the Western Block of NCC; (3) The widely-distributed bodies of early Palaeoproterozoic orthogneisses in the Khondalite Belt might be one of the important sources for detritus material in the khondalite series; (4) Collision between the Yinshan Block, the Ordos Block and the Eastern Block occurred in the same tectonothermal event of late Palaeoproterozoic, resulting in the final assembly of the NCC.

Khondalite Belt, Palaeoproterozoic, SHRIMP dating, Helan Mountains, North China Craton

Recent progress in understanding of the North China Craton (NCC) is identification of some huge Palaeoproterozoic tectonic belts. Zhao et al.^[1–4] suggested that the Western Block and the Eastern Block collided along the Trans-North China Orogen at the end of Palaeoproterozoic (Figure 1), unifying the NCC. Recently, Zhao et al.^[5] recognised a tectonic belt, named the Khondalite Belt, in the Western Block of the NCC and suggested that it

marked the collision between the Yinshan Mountains Block in the north and the Ordos Block in the south during a period of 2.0–1.9 Ga, earlier than the ~1.85 Ga collision between the Western and Eastern blocks. Wan

Received December 29, 2006; accepted May 29, 2007

doi: 10.1007/s11434-007-0404-9

[†]Corresponding author (email: dongchunyan@sina.com)

Supported by the Key Programs of the Ministry of Land and Resource of China (Grant No.1212010711815) and the Program of Beijing SHRIMP Centre

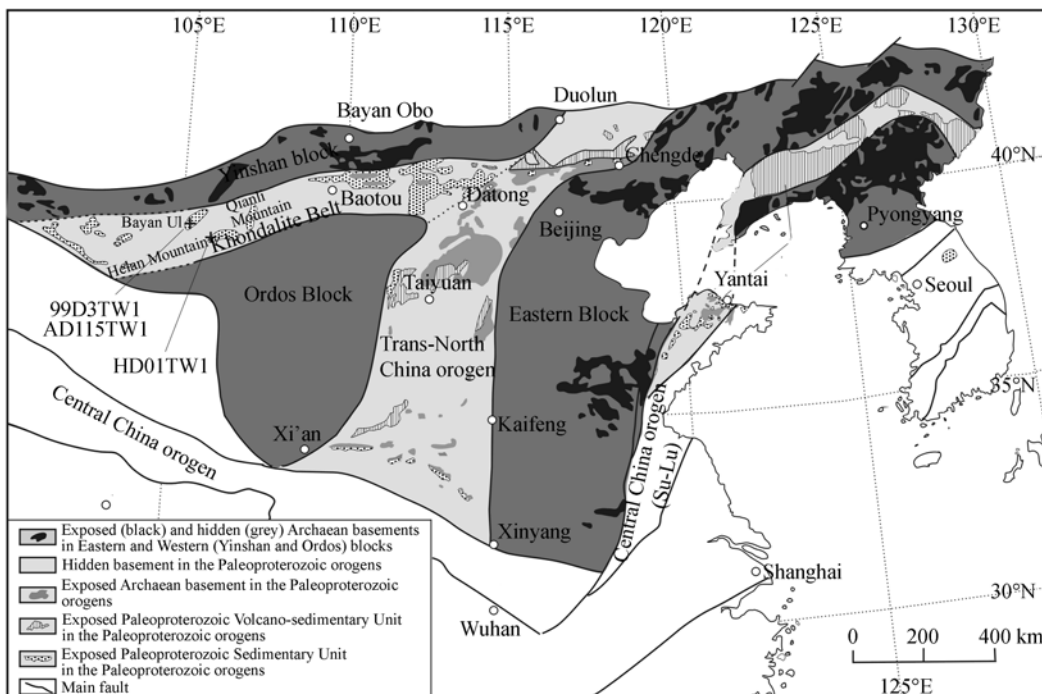


Figure 1 Map of the North China Craton showing the Paleoproterozoic orogenic belts (modified after ref. [1]), showing locations of samples analyzed in this study and by ref. [11].

et al.^[6] considered that all the blocks were assembled in a single complex event, where the Yinshan Mountains and Ordos blocks collided first and then were juxtaposed with the Eastern Block. By applying SHRIMP U-Pb dating technique to the Wulashan Group in the Daqing Mountain area, Wan et al.^[7] obtained metamorphic and detrital zircon ages of 2.4 Ga and 2.5 Ga from one meta-sedimentary sample, and 1.9 Ga and 2.1 Ga from another meta-sedimentary sample, suggesting that there are both early and late Palaeoproterozoic meta-sedimentary rocks in the Khondalite Belt. This paper reports SHRIMP U-Pb dating and Hf isotope analyses of zircons from gneissic granite and garnet-mica two-feldspar gneiss of the Helanshan Group in the Bayan Ul-Helan Mountains area, western portion of the Khondalite Belt. This provides formation ages of the Helanshan Group and associated granitoid rocks, helping to understand the tectonic evolution of the Khondalite Belt as a whole.

1 Geological background and samples

Bayan-Ul is located in the western portion of the Khondalite Belt^[8,9], western Inner Mongolia (Figure 1). The area consists of gneissic quartzofeldspathic rocks with some amphibolite and marble enclaves, all of which in early research were interpreted as Archaean

supracrustal rocks, named Wulashan Group^[10]. However, Li et al.^[11] suggested that the quartzofeldspathic rocks are deformed granodiorites, and therefore interpreted a single zircon TIMS U-Pb age of 2082±22 Ma as their intrusion age. The gneissic granite sample AD115TW1 for this study is from 39°36'29"N and longitude 105°10'4"E, about 30 km northeast of the sample 99D3TW1 analyzed by Li et al.^[11]. The rock is homogenous on the outcrop scale (Figure 2) and consists of plagioclase (48%), quartz (27%), microcline (18%) and biotite (7%). Two portions can be subdivided according to texture and grain size. Main domains consist of coarse-grained plagioclase + quartz + microcline. The



Figure 2 Gneissic granite (AD115TW1) in the Bayan Ul area.

plagioclase shows polysynthetic twinning and is partly sericitized. Quartzes show banded aggregations, with subgrain textures and wavy extinction. Other domains are mainly composed of fine-grained brown biotite + plagioclase+quartz. Both the coarse- and fine-grained domains are distributed as bands as a gneissosity. It is evident that the rock underwent strong deformation and high grade metamorphism.

The Helanshan Group is an important part of the Khondalite Belt, and is located in the Helan Mountains area, about 120 km east of Bayan Ul (Figure 1). It consists mainly of Al-rich gneiss, garnet-biotite fine-grained gneiss, garnet-biotite-plagioclase fine-grained gneiss and marble, all of which carry upper amphibolite-granulite facies metamorphic assemblages. Hu et al.^[12] obtained seven groups of $^{207}\text{Pb}/^{206}\text{Pb}$ zircon evaporation ages, ranging from 2.10 to 1.85 Ga, for sillimanite-cordierite-bearing gneiss and biotite two-feldspar fine-grained gneiss from the Helanshan Group and two groups of $^{207}\text{Pb}/^{206}\text{Pb}$ zircon evaporation ages (1.98 and 1.89 Ga) for garnetiferous granite in the area. They thought that these ages solely recorded a Palaeoproterozoic metamorphic age for the Helanshan Group, and that the rocks formed during the Archaean^[12]. The Helanshan Group garnet-mica two-feldspar gneiss sample HD01TW1 is from 39°23'20"N and, 105°30'49"E. The rock is gneissose and is composed of quartz (27%), K-feldspar (29%), plagioclase (26%), mica (10%) and some garnet. The garnet is unevenly distributed as granular or irregular aggregations. The biotite forms a foliation but most has been altered to chlorite.

2 Analytical techniques

Whole rock major elements, together with Cr to Th and REE plus Y abundances, were determined by XRF and ICP MS at the National Research Center of Geoanalysis in Beijing.

Zircon crystals were extracted from the samples using standard crushing and separation techniques^[13] and U/Pb dating was carried out using the SHRIMP II ion microprobe at Beijing SHRIMP Centre. Analytical procedures were similar to those described by Williams^[14]. The intensity of the primary O⁻² ion beam was 9 nA and the spot sizes were 25–30 μm. Three to four scans through the mass stations were made for detrital zircon with a standard to sample ratio of 1:5. Five scans through the mass stations were made for magmatic and metamorphic

zircons, with a standard to sample ratio of 1:3–4. The standard TEMORA was used for calibration of $^{206}\text{Pb}/^{238}\text{U}$, and U-Th-Pb abundances were determined using SL13. The measured ^{204}Pb was applied to the common lead correction using Pb of Broken Hill galena composition^[15]. Data processing was carried out using the SQUID and ISOPLOT programs^[16]. The errors for individual analyses are quoted at the 1σ level, whereas the errors for weighted mean ages are quoted at 95% confidence level.

In-situ Hf isotopic composition of zircon was measured with a Geolas-193 laser-ablation microprobe, attached to a Neptune multi-collector ICPMS, at Institute of Geology and Geophysics, Chinese Academy of Sciences, in Beijing. The instrumental conditions and analytical procedure were described by Wu et al.^[17,18]. Ablation time was about 26s for 200 cycles of each measurement, with a 8-Hz repetition rate, a laser power of 100 mJ/pulse and a spot size of 63 μm. Zircon standard 91500 was used as the reference ($^{176}\text{Hf}/^{177}\text{Hf} = 0.282306$)^[19]. Zircon 91500 analyzed ($n=8$) in this study yielded $^{176}\text{Lu}/^{177}\text{Hf}_{\text{corr}}$ values of 0.000277–0.000296 (with an average of 0.000283) and $^{176}\text{Hf}/^{177}\text{Hf}_{\text{corr}}$ values of 0.282259–0.282304 (with an average of 0.282276). Parameters for calculation are as follows: decay constant for ^{176}Lu is $1.865 \times 10^{-11} \text{ a}^{-1}$ ^[20], chondritic ratios of $^{176}\text{Hf}/^{177}\text{Hf}$ and $^{176}\text{Lu}/^{177}\text{Hf}$ are 0.0332 and 0.282772^[21], and $^{176}\text{Hf}/^{177}\text{Hf}$ of present-day depleted mantle is 0.28325^[22]. Following the practice of Zheng et al.^[23–25], initial Hf isotope ratios for zircons from metamorphic rocks were calculated at different ages for core, mantle and rim, respectively; one-stage model Hf was calculated relative to the depleted mantle reservoir whereas two-stage model Hf age relative to average continental crust reservoir.

3 Geochemistry

Gneissic granite (AD115TW1) is high in SiO₂ (70.86%) and K₂O (4.48%) and low in Na₂O (3.14%), with a low REE content ($\Sigma\text{REE}=80.7$ ppm), strong fractionation between HREE and LREE ((La/Yb)_n=34.7) and strong positive Eu anomaly (Eu/Eu*=4.0) (Table 1, Figure 3(a)). It is relatively enriched in large ion lithophile elements (LILE), weakly depleted in the high field strength elements (HFSE) Nb and P and depleted in the compatible element Cr (Figure 3(b)). Melt extraction by anatexis may be one of the reasons for the low REE composition

Table 1 Element compositions of rocks from the Bayan Ul-Helan Mountains area^{a)}

No.	1	2	3
Sample No.	AD115TW1	99D3TW1	HD01TW1
Rock type	Gneissic granite	Gneissic granodiorite	Garnet-mica two-feldspar gneiss
Location	Bayan Ul	Bayan Ul	Helan Mountains
SiO ₂	70.86	63.43	73.09
TiO ₂	0.33	0.57	0.51
Al ₂ O ₃	13.69	17.32	13.12
Fe ₂ O ₃	0.96	0.99	0.38
FeO	1.83	2.75	2.91
MnO	0.04	0.09	0.04
MgO	0.99	1.34	1.57
CaO	2.03	2.85	0.48
Na ₂ O	3.14	3.67	1.98
K ₂ O	4.48	3.80	3.86
P ₂ O ₅	0.08	0.11	0.05
H ₂ O ⁺	1.06	1.74	1.40
CO ₂	0.73	0.73	0.21
Total	100.22	99.39	99.60
Cr	16		52
Sc	3.3		7.1
Rb	77	130	
Ba	950	949	
Sr	524	207	
Nb	7.0	16	
Ta	0.30	0.72	
Hf	3.4	7.5	
Zr	130	274	
Y	3.1	20	
Th	2.0	13	
U	0.58	0.95	
La	20.0	39.7	41.5
Ce	29.8	65.26	79.7
Pr	3.08	7.17	9.51
Nd	21.6	25.22	35.5
Sm	1.46	4.39	5.82
Eu	1.84	1.63	1.31
Gd	1.30	4.45	5.02
Tb	0.13	0.59	0.69
Dy	0.55	2.97	3.72
Ho	0.10	0.56	0.71
Er	0.35	1.38	2.14
Tm	0.05	0.2	0.29
Yb	0.38	1.21	2.07
Lu	0.06	0.19	0.32
Σ REE	80.7	154.9	188.3
(La/Yb) _n	34.7	21.6	13.2
Eu/Eu*	4.0	1.1	0.73

a) Sample 99D3TW1 is from ref. [11], major element in %, REE and trace element in ppm.

of the rock with the positive Eu anomaly relating to accumulated residual plagioclase. Gneissic granodiorite (99D3TW1) analysed by Li et al.^[11] is relatively low in

SiO₂ (63.43%), with similar K₂O and Na₂O contents (3.80% and 3.67%, respectively). It shows a relatively high REE content (Σ REE=154.9 ppm), weak HREE and LREE fractionation ((La/Yb)_n=21.6) and an obvious Eu anomaly (Eu/Eu*=1.1) (Table 1, Figure 3(a)). The geochemical difference between samples AD115TW1 and 99D3TW1 indicates that they represent different intrusions or had different in situ melting histories superimposed.

Garnet-mica two-feldspar gneiss (HD01TW1) is high in SiO₂ (73.09%) and K₂O (3.86%) and low in Na₂O (1.98%), with a high REE content (Σ REE=188.3 ppm), weak HREE and LREE fractionation ((La/Yb)_n=13.2) and negative Eu anomaly (Eu/Eu*=0.73) (Table 1, Figure 3(a)). In Pearce diagram, it is enriched in LILE elements and depleted in HFSE elements such as Nb, P and Ti (Figure 3(b)). The rock shows high maturity, being similar in chemical feature to post Archaean sedimentary rocks^[26].

4 Zircon petrography and U-Pb ages

Zircons from gneissic granite sample (AD115TW1) are columnar and stubby in shape and commonly show core-mantle-rim structures in cathodoluminescence (CL) images (Figure 4(a), (b)), with the mantle and rim varying in width. The cores usually show oscillatory zoning with some being homogenous. The mantles are homogenous in texture in CL images. They embay the cores, thus showing recrystallization features. The rims are also homogenous but show weaker luminescence in CL and are interpreted as being metamorphic in origin. Totally, 27 analyses were made on 18 zircon grains. The analyses of 8 spots on core domains show ranges of U and Th contents and Th/U ratios from 37 to 307 ppm, 13–107 ppm and 0.26–0.89 (Table 2), respectively. They commonly show distinct lead loss, but with spot 6.2C showing reverse discordance. Excepting 1.2C which shows the most distinct lead loss, the remaining seven spots give a weighted mean $^{207}\text{Pb}/^{206}\text{Pb}$ age of 2323 ± 20 Ma (MSWD = 1.9), that is interpreted as the formation age of the granite. The analyses of 7 spots on mantle domains have U and Th contents of 134–272 and 33–81 ppm, respectively, and Th/U ratios of 0.23–0.36. They show a large variation in $^{207}\text{Pb}/^{206}\text{Pb}$ age, with a weighted mean $^{207}\text{Pb}/^{206}\text{Pb}$ age of 1923 ± 28 Ma (MSWD=4.2). Some mantle ages might be mixtures

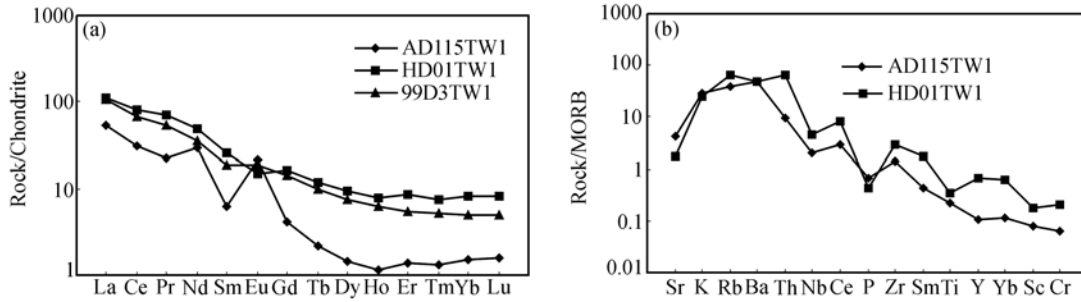


Figure 3 REE patterns (a) and Spider diagrams (b) of rocks from the Bayan Ul-Helan Mountains area. AD115TW1, Gneissic granite; 99D3TW1, gneissic granodiorite; HD01TW1, garnet-mica two-feldspar gneiss.

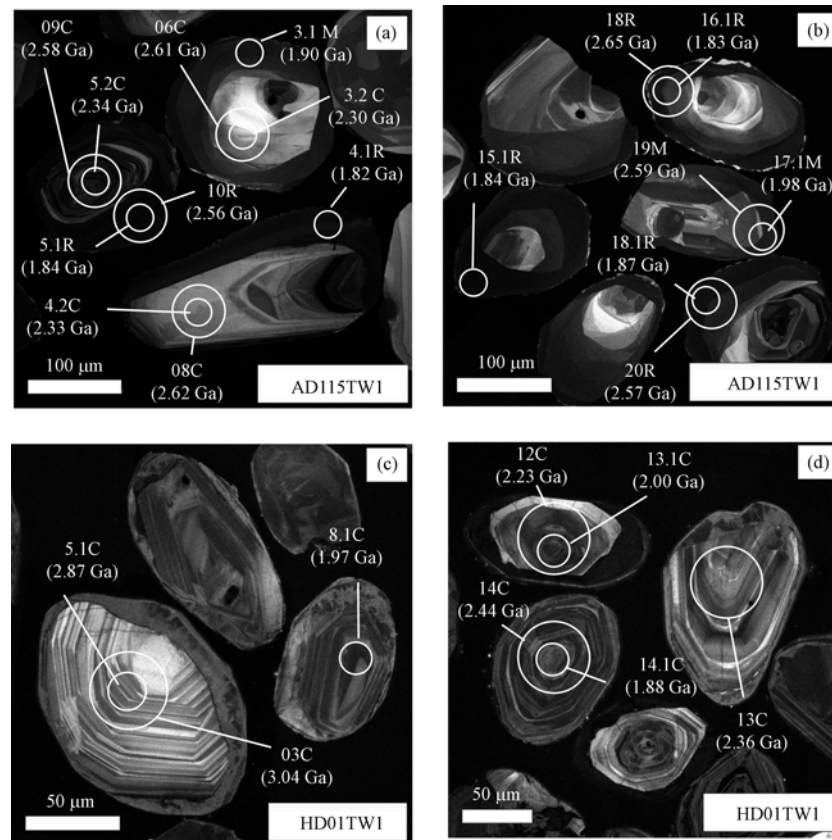


Figure 4 CL images of zircons from gneissic granite (AD115TW1) and garnet-mica two-feldspar gneiss (HD01TW1) in the Bayan Ul-Helan Mountains area. Ellipse (~30 µm) and circle (~60 µm) show positions of SHRIMP U-Pb and ICP-MS Hf analytical sites with their identification numbers as in Tables 2 and 3, respectively.

because the spot straddled into cores or rims when dating the mantles. Furthermore, the mantles commonly show distinct lead loss. Therefore, the age of 1923 ± 28 Ma is likely to only approximate the age of the mantles. 12 analyses on rim domains show ranges of U and Th contents and Th/U ratios from 209 to 1239 ppm, 50–299 ppm and 0.20–0.52 (Table 2), respectively. Some rims also show distinct loss of radiogenic lead. Five spots with the weakest lead loss (1.1R, 5.1R, 13.1R, 18.1R and 21.1R) give a weighted mean $^{207}\text{Pb}/^{206}\text{Pb}$ age

of 1856 ± 12 Ma (MSWD=1.0) (Figure 5(a)), being interpreted as timing a Palaeoproterozoic metamorphic event.

Zircons from garnet-mica two-feldspar gneiss (HD01TW1) are stubby or rounded in shape and show core-rim structures in CL images (Figure 4(c), (d)). However, only a few of the overgrowth rims are wide enough to be analysed. The relationships between outer shape and inner texture clearly show their detrital origin, consistent with the interpretation that the protolith of the

Table 2 SHRIMP U-Pb ages of zircons from the Bayan Ul-Helan Mountains area^{a)}

Spot	$^{206}\text{Pb}^*$ (%)	U (ppm)	Th (ppm)	$^{232}\text{Th}/^{238}\text{U}$	$^{206}\text{Pb}^*$ (ppm)	$^{207}\text{Pb}^*/^{206}\text{Pb}^*$	$\pm\%$	$^{207}\text{Pb}^*/^{235}\text{U}$	$\pm\%$	$^{206}\text{Pb}^*/^{238}\text{U}$	$\pm\%$	Error	$^{206}\text{Pb}/^{238}\text{U}$ age (Ma)	$^{207}\text{Pb}/^{206}\text{Pb}$ age (Ma)	$^{208}\text{Pb}/^{232}\text{Th}$ age (Ma)	Discordant (%)
Gneissic granite in the Bayan Ul area (AD115TW1)																
1.1R	0.03	247	61	0.25	65.2	0.1137	1.5	4.81	2.4	0.3069	1.8	0.759	1725 ± 27	1859 ± 28	1673 ± 36	7
1.2C	0.08	76	45	0.61	21.2	0.1291	1.1	5.78	2.0	0.3245	1.7	0.836	1812 ± 27	2086 ± 20	1817 ± 53	13
2.1C	0.06	100	76	0.79	33.6	0.1453	0.81	7.86	1.8	0.3926	1.6	0.890	2135 ± 29	2291 ± 14	2155 ± 39	7
2.2R	0.21	369	105	0.30	91.6	0.11247	0.66	4.467	1.6	0.2881	1.5	0.914	1632 ± 21	1840 ± 12	1640 ± 35	11
3.1M	0.02	220	55	0.26	55.3	0.1165	1.3	4.694	2.0	0.2922	1.5	0.773	1653 ± 23	1903 ± 23	1704 ± 34	13
3.2C	0.23	37	16	0.44	13.2	0.1457	1.5	8.41	2.4	0.4185	1.9	0.781	2253 ± 36	2296 ± 26	2074 ± 77	2
4.1R	0.02	390	119	0.32	93.5	0.11152	0.58	4.29	2.5	0.2787	2.4	0.973	1585 ± 34	1824 ± 10	1681 ± 47	13
4.2C	0.13	48	42	0.89	18.0	0.1487	1.2	8.87	2.1	0.4326	1.8	0.820	2317 ± 34	2331 ± 21	2419 ± 53	1
5.1R	0.02	457	231	0.52	125	0.11231	0.72	4.94	2.2	0.3188	2.0	0.943	1784 ± 32	1837 ± 13	1888 ± 40	3
5.2C	0.03	307	107	0.36	128	0.14920	0.48	9.93	1.6	0.4829	1.5	0.954	2540 ± 32	2337 ± 8.2	2822 ± 76	-9
6.1M	0.03	265	60	0.23	66.6	0.11665	0.65	4.700	1.7	0.2922	1.5	0.920	1653 ± 22	1905 ± 12	1656 ± 37	13
6.2C	0.11	69	37	0.55	22.1	0.1468	1.1	7.49	2.1	0.3702	1.7	0.839	2031 ± 30	2308 ± 19	2182 ± 74	12
7.1R	0.02	386	105	0.28	93.8	0.11372	0.59	4.434	1.6	0.2828	1.5	0.929	1606 ± 21	1860 ± 11	1675 ± 29	14
7.2M	0.03	272	60	0.23	74.5	0.11643	0.64	5.121	1.6	0.3190	1.5	0.920	1785 ± 23	1902 ± 11	1861 ± 35	6
8.1R	0.07	314	62	0.20	75.1	0.11310	0.70	4.340	1.7	0.2783	1.5	0.907	1583 ± 21	1850 ± 13	1730 ± 35	14
8.2C	0.08	54	18	0.35	18.1	0.1497	1.1	8.01	2.3	0.3882	2.0	0.866	2114 ± 36	2342 ± 20	2133 ± 63	10
9.1R	0.05	279	68	0.25	62.9	0.11265	0.71	4.074	1.7	0.2623	1.5	0.905	1502 ± 20	1843 ± 13	1498 ± 29	18
9.2C	0.11	52	13	0.26	15.7	0.1459	1.6	7.07	2.4	0.3515	1.7	0.727	1942 ± 29	2298 ± 28	1894 ± 64	16
10.1M	0.05	208	52	0.26	49.7	0.11696	0.77	4.494	1.7	0.2787	1.5	0.892	1585 ± 21	1910 ± 14	1600 ± 32	17
11.1M	0.04	196	54	0.28	48.2	0.11946	0.78	4.696	1.7	0.2851	1.6	0.895	1617 ± 22	1948 ± 14	1693 ± 34	17
12.1M	0.08	134	33	0.25	33.8	0.1183	1.8	4.79	2.5	0.2938	1.6	0.661	166 ± 24	1931 ± 33	1734 ± 45	14
13.1R	0.06	209	50	0.25	53.3	0.1142	0.96	4.668	1.8	0.2966	1.6	0.853	1674 ± 23	1866 ± 17	1734 ± 41	10
14.1R	0.01	542	170	0.32	123	0.1123	1.6	4.089	2.2	0.2642	1.5	0.695	1511 ± 20	1836 ± 28	1608 ± 28	18
15.1R	0.00	381	120	0.32	84.2	0.11247	0.68	3.985	1.7	0.2569	1.6	0.916	1474 ± 21	1840 ± 12	1503 ± 28	20
16.1R	0.07	245	59	0.25	53.0	0.11186	0.79	3.890	1.7	0.2522	1.5	0.888	1450 ± 20	1830 ± 14	1476 ± 31	21
17.1M	0.14	230	81	0.36	59.9	0.1216	0.83	5.072	1.7	0.3025	1.5	0.879	1703 ± 23	1980 ± 15	2029 ± 58	14
18.1R	0.00	336	97	0.30	96.2	0.11421	0.56	5.248	1.6	0.3332	1.5	0.938	1854 ± 24	1867 ± 10	1925 ± 33	1
Garnet-mica two-feldspar gneiss in the Helan Mountains area (HD01TW1)																
1.1R	2.70	2276	182	0.08	215	0.0880	2.9	1.291	6.6	0.1065	5.9	0.898	652 ± 37	1381 ± 56	915 ± 180	53
2.1R	0.18	1522	19	0.01	131	0.07843	0.89	1.085	6.1	0.1003	6.0	0.989	616 ± 35	1158 ± 18	687 ± 170	47
3.1R	4.00	1368	22	0.02	85.8	0.0801	3.6	0.771	7.1	0.0699	6.2	0.866	435 ± 26	1199 ± 71	2877 ± 500	64
4.1C	0.04	136	99	0.75	54.0	0.1217	1.4	7.77	6.0	0.463	5.9	0.974	2455 ± 120	1981 ± 25	2297 ± 140	-24
5.1C	0.12	57	29	0.53	23.9	0.2056	1.4	13.88	6.1	0.490	5.9	0.972	2569 ± 130	2871 ± 23	2603 ± 160	11
6.1C	0.17	114	75	0.68	32.0	0.1214	1.7	5.47	6.1	0.327	5.9	0.960	1822 ± 93	1976 ± 31	1925 ± 120	8
7.1C	0.14	162	102	0.65	39.7	0.1206	1.5	4.73	6.0	0.285	5.8	0.968	1615 ± 84	1965 ± 27	1526 ± 94	18
8.1C	0.00	185	167	0.93	52.3	0.1211	1.2	5.49	6.0	0.329	5.9	0.981	1833 ± 93	1972 ± 21	1986 ± 120	7
9.1C	0.00	95	58	0.63	28.8	0.1245	1.6	6.04	6.1	0.352	5.9	0.965	1943 ± 98	2022 ± 28	2061 ± 130	4
10.1C	0.01	477	233	0.51	62.8	0.1098	1.1	2.32	5.9	0.1533	5.8	0.982	919 ± 50	1797 ± 21	705 ± 54	49
11.1C	0.01	239	175	0.76	92.5	0.1613	1.6	9.99	6.1	0.449	5.9	0.963	2392 ± 120	2469 ± 28	2356 ± 140	3
12.1C	0.06	149	110	0.76	46.6	0.1238	1.4	6.19	6.0	0.363	5.9	0.974	1995 ± 100	2012 ± 24	2138 ± 130	1
13.1C	0.35	237	115	0.50	48.3	0.1228	1.9	4.00	6.1	0.236	5.8	0.953	1368 ± 72	1998 ± 33	1912 ± 120	32
14.1C	0.25	177	142	0.83	39.3	0.1150	1.8	4.08	6.1	0.258	5.9	0.957	1478 ± 78	1880 ± 32	1464 ± 91	21
15.1C	0.14	319	78	0.25	63.9	0.1192	1.3	3.82	6.0	0.233	5.8	0.975	1348 ± 71	1945 ± 24	1477 ± 95	31
16.1C	0.09	428	226	0.55	71.4	0.1098	1.2	2.93	6.0	0.194	5.8	0.980	1142 ± 61	1796 ± 22	1738 ± 100	36
17.1C	0.00	161	50	0.32	37.1	0.1193	1.4	4.40	6.0	0.268	5.9	0.972	1529 ± 80	1946 ± 25	1736 ± 110	21

a) Pb^* means radiogenic lead. For gneissic granite (AD115TW1), C, M and R denote core (magmatic), mantle (metamorphic) and rim (metamorphic) zircons, respectively; For garnet-mica two-feldspar gneiss (HD01TW1), C and R denote core (detrital) and rim (metamorphic) zircons, respectively.

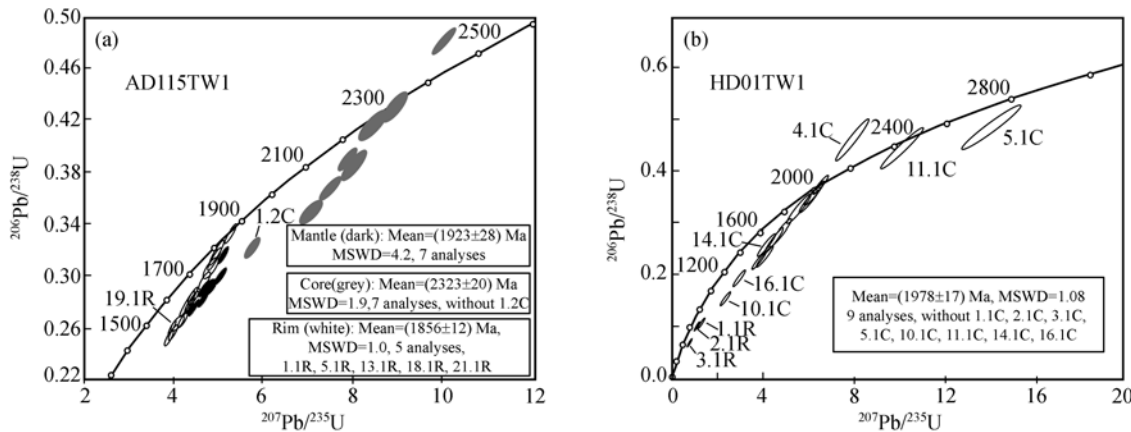


Figure 5 Concordia diagram of SHRIMP U-Pb data for zircons from gneiss granite (AD115TW1) (a) and garnet-mica two-feldspar gneiss (HD01TW1) (b) in the Bayan Ul-Helan Mountains area.

rock is sediment. 14 analyses on detrital core domains show ranges of U and Th contents and Th/U ratios from 57 to 477 ppm, 58–233 ppm and 0.25–0.93 (Table 2), respectively. Excepting 5.1C and 11.1C which are Archaean (2871 and 2469 Ma), all spots are distributed along a discordia with an upper intercept age of ~2.0 Ga. Of them, 9 spots with the weakest lead loss give a weighted mean $^{207}\text{Pb}/^{206}\text{Pb}$ age of 1978 ± 17 Ma ($\text{MSWD} = 1.1$) (Figure 5(b)). This age represents the formation age of the main source from which the detrital material was derived. This also constrains the maximum age of deposition of the sediment. No precise metamorphic age has been determined for the reason that the overgrowth rim is very high in U content, resulting in distinct lead loss. Three analyses on the rim give low Th/U ratios (0.01–0.08), a feature of metamorphic zircon.

5 Hf isotope compositions of zircons

A total of 20 analyses were made on 14 zircon grains from gneissic granite sample (AD115TW1) for Lu-Hf isotopes (Table 3). Among them, eight analyses on cores have $\varepsilon_{\text{Hf}}(t)$ ($t=2323$ Ma, the weighted mean $^{207}\text{Pb}/^{206}\text{Pb}$ age of the core), T_{DM1} and T_{DM2} ages ranging from 0.21 to 2.02, 2585 to 2652 Ma and 2658 to 2812 Ma, respectively. The analyses of 4 spots on mantles have $\varepsilon_{\text{Hf}}(t)$ ($t=1923$ Ma, the weighted mean $^{207}\text{Pb}/^{206}\text{Pb}$ age of the mantle), T_{DM1} and T_{DM2} ages ranging from –8.31 to –3.67, 2455 to 2631 Ma and 2623 to 2854 Ma, respectively. The analyses of 7 spots on rims have $\varepsilon_{\text{Hf}}(t)$ ($t=1856$ Ma, the weighted mean $^{207}\text{Pb}/^{206}\text{Pb}$ age of the rim), T_{DM1} and T_{DM2} ages ranging from –10.47 to –5.55, 2472 to 2655 Ma and 2516 to 2908 Ma, respectively.

Most of the cores, mantles and rims are very similar in Hf isotope compositions, roughly showing linear relationship between $^{207}\text{Pb}/^{206}\text{Pb}$ age and $\varepsilon_{\text{Hf}}(t)$ diagram (Figure 6(a)). However, some mantle and rim analyses show high $^{176}\text{Hf}/^{177}\text{Hf}_{(\text{c})}$ ratio, with AD115TW1-03R being 0.281604.

Nineteen spots were analyzed on 19 zircon grains from garnet-mica two-feldspar gneiss sample HD01TW1 for Lu-Hf isotopes (Table 3). Among 18 spots on detrital cores, 16 of them have $\varepsilon_{\text{Hf}}(t)$ ($t=1978$ Ma, the weighted mean $^{207}\text{Pb}/^{206}\text{Pb}$ age of the most cores), T_{DM1} and T_{DM2} ranging from –13.6 to 9.54, 1999 to 3047 Ma and 2005 to 3159 Ma, respectively. The analyses of detrital zircons show large variations in $^{207}\text{Pb}/^{206}\text{Pb}$ age vs. $\varepsilon_{\text{Hf}}(t)$ diagram (Figure 6(b)). Six analyses on detrital zircons with $^{207}\text{Pb}/^{206}\text{Pb}$ ages of ~2.0 Ga have $\varepsilon_{\text{Hf}}(t)$ (t is the $^{207}\text{Pb}/^{206}\text{Pb}$ age at Hf isotope analysis sites) ranging from –3.32 to 4.48. The detrital cores HD01TW1-03C and HD01TW1-11C have the $^{207}\text{Pb}/^{206}\text{Pb}$ ages of 2871 Ma and 2469 Ma, with their $\varepsilon_{\text{Hf}}(t)$ (t is the $^{207}\text{Pb}/^{206}\text{Pb}$ age at Hf isotope analysis sites), T_{DM1} and T_{DM2} ages of –3.57 and 2.29/3047 Ma and 2921 Ma/3097 Ma and 3056 Ma, respectively. The only analysis on rim in this study gives a T_{DM1} age of 2453 Ma and a T_{DM2} age of 2500 Ma.

6 Discussions and conclusions

Li et al.^[11] determined the single zircon TIMS U-Pb age of gneissic granodiorite (99D3TW1) in the Bayan Ul area to be 2.08 Ga and suggested that the widely-distributed gneissose granodiorites formed during the Palaeoproterozoic period, not Archaean, as previously considered. This study further supports this interpretation,

Table 3 Hf isotope compositions of zircons from the Bayan-Ul-Helan Mountains area^{a)}

No.	Spot	$^{207}\text{Pb}/^{206}\text{Pb}$ age (Ma)	$^{176}\text{Yb}/^{177}\text{Hf}$	$^{176}\text{Lu}/^{177}\text{Hf}$	$^{176}\text{Hf}/^{177}\text{Hf}_{(\text{c})}$	2σ	$\varepsilon_{\text{Hf}}(0)$	$\varepsilon_{\text{Hf}}(t_1)$	$\varepsilon_{\text{Hf}}(t_2)$	$\varepsilon_{\text{Hf}}(t_3)$	2 s	$T_{\text{DM1}}(\text{Ma})$	$T_{\text{DM2}}(\text{Ma})$	$f_{\text{Lu/Hf}}$
Gneissic granite in the Bayan Ul area (AD115TW1)														
01C	1.2C	2086	0.025486	0.000449	0.281333	0.000018	-50.90	-4.93	0.44	0.44	0.65	2643	2812	-0.99
02R	1.1R	1859	0.024874	0.000607	0.281370	0.000021	-49.58	-8.91	1.52	-8.97	0.76	2603	2825	-0.98
03R		0.027513	0.000744	0.281604	0.000032	-41.30		9.63	-0.83	1.12	2294	2285	-0.98	
04R	2.2R	1840	0.016352	0.000317	0.281341	0.000023	-50.62	-10.02	0.93	-9.66	0.82	2623	2865	-0.99
05C	2.1C	2291	0.030440	0.000581	0.281332	0.000021	-50.92	-0.51	0.21	0.21	0.74	2652	2761	-0.98
06 C	3.2C	2296	0.021771	0.000362	0.281351	0.000020	-50.24	0.62	1.24	1.24	0.69	2612	2709	-0.99
07M		0.024706	0.000498	0.281360	0.000023	-49.92		1.35	-7.68	0.83	2609	2695	-0.99	
08C	4.2C	2331	0.021358	0.000372	0.281347	0.000019	-50.39	1.26	1.08	1.08	0.67	2618	2706	-0.99
09C	5.2C	2337	0.045610	0.000803	0.281393	0.000018	-48.77	2.34	2.02	2.02	0.63	2585	2658	-0.98
10R	5.1R	1837	0.025356	0.000567	0.281399	0.000023	-48.56	-8.33	2.60	-7.90	0.83	2561	2779	-0.98
11C	6.2C	2308	0.019363	0.000339	0.281353	0.000024	-50.20	0.98	1.32	1.32	0.87	2609	2701	-0.99
12M	6.1M	1905	0.022530	0.000426	0.281471	0.000028	-46.02	-4.08	5.38	-3.67	1.00	2455	2623	-0.99
13C		0.017114	0.000308	0.281325	0.000019	-51.16		0.40	0.40	0.67	2643	2742	-0.99	
14M	7.2M	1902	0.021900	0.000391	0.281339	0.000017	-50.69	-8.78	0.75	-8.31	0.59	2631	2854	-0.99
15C	8.2C	2342	0.014406	0.000306	0.281351	0.000017	-50.27	1.73	1.30	1.30	0.61	2609	2692	-0.99
16R	8.1R	1850	0.022854	0.000548	0.281347	0.000021	-50.39	-9.85	0.80	-9.71	0.74	2630	2864	-0.98
17R		0.026894	0.000576	0.281465	0.000023	-46.20		4.96	-5.55	0.82	2472	2516	-0.98	
18R	16.1R	1830	0.019540	0.000375	0.281320	0.000018	-51.36	-11.06	0.10	-10.47	0.65	2655	2908	-0.99
19M	17.1M	1980	0.032398	0.000644	0.281380	0.000022	-49.23	-5.89	1.82	-7.17	0.77	2589	2770	-0.98
20R	18.1R	1867	0.016419	0.000310	0.281382	0.000022	-49.16	-7.94	2.41	-8.19	0.77	2565	2780	-0.99
Garnet-mica two-feldspar gneiss in the Helan Mountains area (HD01TW1)														
No.	Spot	$^{207}\text{Pb}/^{206}\text{Pb}$ age (Ma)	$^{176}\text{Yb}/^{177}\text{Hf}$	$^{176}\text{Lu}/^{177}\text{Hf}$	$^{176}\text{Hf}/^{177}\text{Hf}_{(\text{c})}$	2σ	$\varepsilon_{\text{Hf}}(0)$	$\varepsilon_{\text{Hf}}(t_1)$	$\varepsilon_{\text{Hf}}(t_2)$	$\varepsilon_{\text{Hf}}(t_3)$	2 s	$t_{\text{DM1}}(\text{Hf})$	$t_{\text{DM2}}(\text{Hf})$	$f_{\text{Lu/Hf}}$
01R	1.1R	1381	0.304466	0.008042	0.281827	0.000056	-33.41	-10.21	0.06	2.00	2456	2502	-0.76	
02C		0.071115	0.001372	0.281761	0.000037	-35.75		6.62	1.32	2114	2151	-0.96		
03C	5.1C	2871	0.054848	0.001084	0.281068	0.000029	-60.26	2.29	-17.62	1.03	3047	3097	-0.97	
04C	7.1C	1965	0.079192	0.001697	0.281637	0.000029	-40.12	1.52	1.80	1.04	2305	2394	-0.95	
05C	6.1C	1976	0.066027	0.001105	0.281573	0.000030	-42.39	0.26	0.31	1.05	2358	2466	-0.97	
06C		0.127243	0.001934	0.281790	0.000023	-34.74		6.89	0.83	2105	2137	-0.94		
07C		0.089367	0.001657	0.281513	0.000037	-44.53		-2.57	1.33	2477	2608	-0.95		
08C		0.022109	0.000336	0.281149	0.000022	-57.39		-13.73	0.79	2881	3159	-0.99		
09C		0.035791	0.000636	0.281253	0.000024	-53.73		-10.45	0.85	2763	2997	-0.98		
10C		0.062065	0.001125	0.281834	0.000026	-33.18		9.54	0.93	1999	2005	-0.97		
11C	11.1C	2469	0.033864	0.000588	0.281133	0.000029	-57.95	-3.57	-14.63	1.02	2921	3056	-0.98	
12C	13.1C	1998	0.090571	0.002105	0.281707	0.000038	-37.65	4.17	3.74	1.35	2232	2290	-0.94	
13C		0.031738	0.000718	0.281554	0.000025	-43.06		0.15	0.88	2360	2473	-0.98		
14C	14.1C	1880	0.135735	0.002797	0.281592	0.000033	-41.72	-3.32	-1.27	1.19	2440	2565	-0.92	
15C		0.044575	0.000786	0.281783	0.000032	-34.99		8.17	1.14	2052	2074	-0.98		
16C		0.057303	0.001243	0.281608	0.000032	-41.16		1.37	1.15	2318	2412	-0.96		
17C	10.1C	1797	0.036306	0.000742	0.281652	0.000032	-39.62	-0.46	3.58	1.14	2229	2356	-0.98	
18C	9.1C	2022	0.072834	0.001194	0.281667	0.000029	-39.08	4.48	3.51	1.02	2234	2294	-0.96	
19C		0.077094	0.001223	0.281577	0.000033	-42.27		0.27	1.17	2361	2467	-0.96		

a) $^{176}\text{Hf}/^{177}\text{Hf}_{(\text{c})}$ is $^{176}\text{Hf}/^{177}\text{Hf}$ corrected by standard 95100. Number in the second column is the SHRIMP dating number the same as in Table 2. Age is in Ma. For both samples AD115TW1 and HD01TW1, t_1 in $\varepsilon_{\text{Hf}}(t_1)$ is the age of locations where Hf isotope compositions were analysed, namely the age listed in the third column. For gneissic granite sample (AD115TW1), t_2 in $\varepsilon_{\text{Hf}}(t_2)$ is the weighted mean $^{207}\text{Pb}/^{206}\text{Pb}$ age (2323 Ma) of the core, and t_3 in $\varepsilon_{\text{Hf}}(t_3)$ is the weighted mean $^{207}\text{Pb}/^{206}\text{Pb}$ ages of the core, mantle and rim of zircons (2323 Ma, 1923 Ma and 1856 Ma), respectively. For garnet-mica two-feldspar gneiss (HD01TW1), t_2 in $\varepsilon_{\text{Hf}}(t_2)$ is the weighted mean $^{207}\text{Pb}/^{206}\text{Pb}$ age of the detrital zircons (1978 Ma). T_{DM1} and T_{DM2} are single-stage and two-stage model Hf ages, respectively.

but has revealed more complexity. The core and mantle of zircons from gneiss granite (AD115TW1) give the ages of 2.32 ± 0.02 Ga and 1.92 ± 0.03 Ga, respectively. Therefore, we prefer that the ages of 2.32 ± 0.02 Ga and

1.92 ± 0.03 Ga represent the formation and the first metamorphic age for the granite. The age of 1.86 ± 0.01 Ga of the metamorphic overgrowth rim records the second important later tectonothermal event. Thus it seems

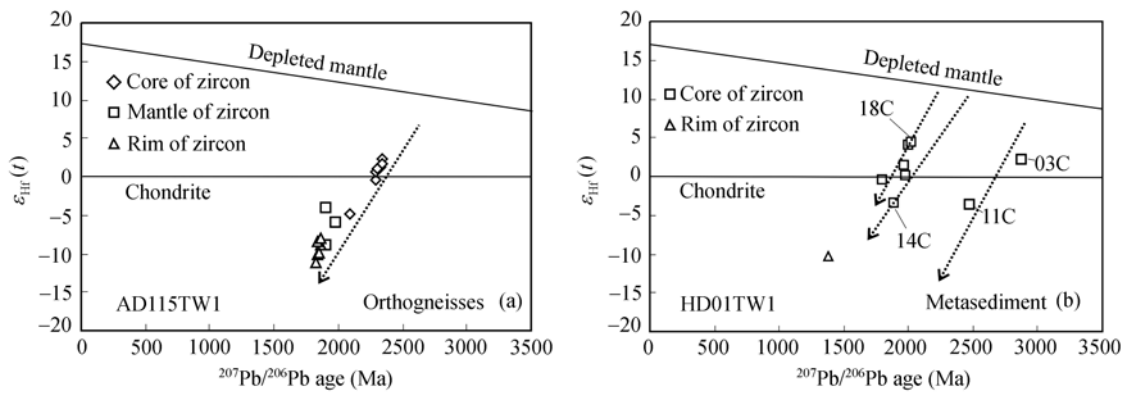


Figure 6 $^{207}\text{Pb}/^{206}\text{Pb}$ age vs. $\epsilon_{\text{Hf}}(t)$ diagrams of zircons from gneissic granite (AD115TW1) and garnet-mica two-feldspar gneiss (HD01TW1) in the Bayan Ul-Helan Mountainss area. SHRIMP U-Pb dating and MC-ICPMS Lu-Hf analyses are made at the same sites.

possible that the zircon age of 2.08 Ga obtained by Li et al.^[11] on the gneissic granodiorite (99DTW1) could be a mixture age of magmatic and metamorphic zircon. The core, mantle and rim of the zircons from gneiss granite (AD115TW1) show some variations in U-Pb age, but their Hf isotope compositions are similar to each other. This is quite different from the zircons from Triassic ultra-high pressure rocks in the Dabie area. In the later, compared with cores, more radiogenic Hf isotopes were incorporated into rims. The newly added radiogenic Hf in the metamorphic rims is considered to be related to the simultaneous formation of HREE-rich garnet, which forms a medium of metamorphic fluid that has a high $^{186}\text{Hf}/^{187}\text{Hf}$ ratio but low Lu/Hf ratio, thus resulting in a high $^{186}\text{Hf}/^{187}\text{Hf}$ ratio and low Lu/Hf ratio for the zircon rim^[23]. In contrast, no garnet and other abundant minerals with high HREE content formed in the gneissic granite in the Bayan Ul area during the metamorphic process. In general, therefore, both the core and rim do not show obvious difference in Hf isotope composition. However, analysis AD115TW1-03R is as high as 0.281604 in $^{176}\text{Hf}/^{177}\text{Hf}_{(\text{c})}$ ratio, with a $\epsilon_{\text{Hf}}(2323 \text{ Ma})$ value of 9.63 and a T_{DM1} age of 2294 Ma, probably indicating the presence of juvenile crust^[24]. Magmatic core zircons usually show the positive $\epsilon_{\text{Hf}}(2.32 \text{ Ga})$ values of 0.21 to 2.02 and T_{DM1} ages of 2585 to 2652 Ma. Te T_{DM1} age is only ~ 300 Ma older than the formation age of the granite, indicating that the granite formed by partial melting of relatively juvenile crust^[27].

The Helanshan Group in the Helan Mountainss area, being similar in rock association and metamorphic grade to the typital Khondalite series of India, used to be considered to be Archaean in age^[12]. However, the age of

the analysed detrital zircons from the garnet-mica two-feldspar gneiss (HD01TW1) are mainly ~ 1.98 Ga, and only two are Archaean. The distinct lead loss of the overgrowth rims made it difficult to determine the metamorphic age which must be Palaeoproterozoic, considering other dating, such as AD115TW1 presented here. The single zircon TIMS U-Pb age of 1.85 Ga obtained by Hu et al.^[12] for meta-sedimentary rocks probably recorded a metamorphic age of the Helanshan Group.

Meta-sedimentary rocks of the khondalite series in eastern portion of the Khondalite Belt gave the metamorphic and youngest detrital zircon ages of 1.85 Ga and 2.0 Ga^[6], or 1.84 Ga and 1.81 Ga^[28], respectively. Meta-sedimentary rocks of the khondalite series in central portion of the Khondalite Belt gave the metamorphic and youngest detrital zircon ages of 1.9 Ga and 2.1 Ga, respectively^[7]. Xia et al.^[28,29] considered that all the 2.01–1.84 Ga zircons from meta-sedimentary rocks of the Khondalite Belt are of detrital origin. The metamorphic and youngest detrital zircons of meta-sedimentary rocks of the khondalite series in western portion of the belt give the ages of 1.86 Ga and 1.98 Ga, respectively. Although various researchers obtained somewhat different results and conclusions, it is evident that there is a huge Palaeoproterozoic khondalite belt between the Yinshan Mountains Block and the Ordos Block in the Western Block of the NCC^[5]. Most of the detrital zircons from the khondalites are rounded in shape with high textural maturity^[6,7,28,29], probably indicating that the detritus material had a long residence time in sedimentary systems.

There are abundant detrital zircons of 2.3–2.0 Ga in

the Palaeoproterozoic meta-sedimentary rocks in different parts of the Khondalite Belt extending in east-west direction over 1200 km, with the proportion being higher than that for Archaean detrital zircons^[6,7,28,29]. Recently, Darby and Gehrels^[30] carried out a study on the age distribution of detrital zircons from sedimentary rocks deposited from the Palaeoproterozoic to the Mesozoic, and revealed an important age peak around 2.00–2.06 Ga. Therefore, there must be a large source composed of Palaeoproterozoic igneous rocks which provided detritus material for the sedimentary basin. Xia et al.^[29] suggested that the Ordos massif was a possible source. However, the 2.3–2.0 Ga rocks widely-distributed in the Khondalite Belt^[31,32] might also be one of the sources for the sediments. Furthermore, there are many over 2.0 Ga igneous provinces globally, such as those now in Brazil, western Australia and northern Greenland, that could also contribute detritus of this age. Detailed comparison can provide insights into relationship between the western NCC and other early Precambrian blocks.

Only six Hf analyses were carried out on the ~2.0 Ga detrital zircons from the garnet-mica two-feldspar gneiss (HD01TW1). However, they show a large variation in Hf isotope composition, with $\epsilon_{\text{Hf}}(t)$, T_{DM1} and T_{DM2} being –0.46 to 4.48, 2234 to 2440 Ma and 2294 to 2565 Ma, respectively. Spots HD01TW1-08 and HD01TW1-09 are higher in T_{DM1} (2881 and 2763 Ma) and T_{DM2} (3159 and 2997 Ma), but a possibility that they are older

detrital zircons cannot be excluded because SHRIMP dating was not undertaken on them. For spot HD01TW1-10, on the other hand, $\epsilon_{\text{Hf}}(1.97 \text{ Ga})$ is very high (9.54), and T_{DM1} is very young (2.0 Ga), the detrital zircon was obviously from a juvenile crustal source with in a very short time after extracting from depleted mantle. Although the number of analyses is still less, the Hf isotope compositions of the ~2.0 Ga detrital zircons show that they were mainly derived from a juvenile crustal source formed by extraction from the depleted mantle, a conclusion also reached by Xia et al.^[29] based on study in the Daqing mountain area. The existence of some older detrital zircons implies that some materials came from more ancient source.

The SHRIMP dating of metamorphic zircons from the gneissic granite (AD115TW1) indicated that the Khondalite Belt underwent a tectonothermal event of ~1.85 Ga, being similar to the Trans-North China Orogen. However, an earlier strong tectonothermal event (1.9–1.95 Ga) was also developed in the Khondalite Belt^[6,7], but apparently not in the Trans-North China Orogen^[33]. This may lend support to the contention that all the blocks were assembled in a single complex event, with the Yinchuan Mountains and Ordos blocks colliding first and then being juxtaposed with the Eastern Block^[7].

The authors thank Zhao Guochun, Xia Xiaoping, Wu Fuyuan and Guo Jinghui for their kind help and discussions. Thanks also go to Allen Nutman for his kind comment and making the manuscript readable. We thank two anonymous reviewers and editor for their valuable comments.

- 1 Zhao G C, Peter A C, Simon A W, et al. Metamorphism of basement rocks in the Central Zone of the North China Craton: Implications for Paleoproterozoic tectonic evolution. *Precambrian Res*, 2000, 103: 55–88
- 2 Zhao G C, Simon A W, Peter A C, et al. Archean blocks and their boundaries in the North China Craton: Lithological, geochemical, structural and P-T path constraints and tectonic evolution. *Precambrian Res*, 2001, 107: 45–73
- 3 Zhao G C, Peter A C, Simon A W, et al. High-Pressure Granulites (Retrograded Eclogites) from the Hengshan Complex, North China Craton: Petrology and Tectonic Implications. *J Petrol*, 2001, 42(6): 1141–1170
- 4 Zhao G C, Sun M, Simon A W. Major tectonic units of the North China Craton and their Paleoproterozoic assembly. *Sci China Ser D-Earth Sci*, 2003, 46(1): 45–60
- 5 Zhao G C, Sun M, Simon A W, et al. Late Archean to Paleoproterozoic evolution of the North China Craton: key issues revisited. *Precambrian Res*, 2005, 136: 177–202
- 6 Wan Y S, Song B, Liu D Y, et al. SHRIMP U-Pb zircon geochronology of Palaeoproterozoic metasedimentary rocks in the North China Craton: Evidence for a major Late Palaeoproterozoic tectonothermal event. *Precambrian Res*, 2006, 149: 249–271
- 7 Wan Y S, Liu D Y, Wang Z J, et al. Poly-Metamorphism and Interdigitation of Tectonic Slices With Different Ages: Evidence From the Precambrian Khondalite Belt in the Daqing mountain Area, North China Craton. *American Geophysics Union Con Abs*, 2006, 120
- 8 Shen B F, Luo H, Li S B, et al. Archean Greenstone Belt Geology and Mine in the North China Craton (in Chinese). Beijing: Geological Publishing House, 1994. 1–202
- 9 Bai J, Huang X G, Wang H C, et al., Precambrian Crust Evolution in the North China Craton (in Chinese). Beijing: Geological Publishing House, 1996. 49–50
- 10 Bureau of Geology and Mineral Resources of Nei Mongol Autonomous Region, Rock and Stratum of Nei Mongol Autonomous Region (in Chinese). Wuhan: China University of Geosciences Press, 1996. 114–120

- 11 Li J J, Shen B F, Li H M, et al. Single-zircon U-Pb age of granodioritic gneiss in the Bayan Ul area, western Inner Mongolia. *Geol Bull China* (in Chinese), 2004, 23(12): 1243—1245
- 12 Hu N G, Yang J X, Wang Z B, et al. The Composition and Evolution of Complex in Helan Mountains (in Chinese). Xi'an: Map Publishing House, 1994. 1—59
- 13 Song B, Zhang Y H, Wan Y S, et al. Mount making and procedure of the SHRIMP dating. *Geol Rev* (in Chinese), 2002, 48(supple): 26—30
- 14 Williams I S. U-Th-Pb geochronology by ion microprobe. In: McKibben M A, Shanks W C, Ridley W I, eds. Applications of Microanalytical Techniques to Understanding Mineralizing Processes. *Rev Econ Geol*, 1998, 7: 1—35
- 15 Cumming G L, Richarda J R. Ore lead isotope ratios in a continuously changing earth. *Earth Planet Sci Lett*, 1975, 28: 155—171
- 16 Ludwig K R. Squid 1.02: a user's manual. Berkeley Geochronology Centre, Special Publication 2, 2001. 19
- 17 Wu F Y, Yang Y H, Xie L W, et al. Hf isotopic compositions of the standard zircons and baddeleyites used in U-Pb geochronology. *Chem Geol*, 2006, 234: 105—126
- 18 Yang J H, Wu F Y, Liu X M, et al. Zircon U-Pb ages and Hf isotopes and their geological significance of the Miyun rapakivi granites from Beijing, China. *Acta Petrol Sin* (in Chinese), 2005, 21(6): 1633—1644
- 19 Woodhead J, Hergt J, Shelley M, et al. Zircon Hf-isotope analysis with an excimer laser, depth profiling, ablation of complex geometries, and concomitant age estimation. *Chem Geol*, 2004, 209: 121—135
- 20 Scherer E, Munker C, Mezger K. Calibration of the lutetium-hafnium clock. *Science*, 2001, 293: 683—687
- 21 Blichert-Toft J, Albarede F. The Lu-Hf geochemistry of chondrites and the evolution of the mantle-crust system. *Earth Planet Sci Lett*, 1997, 148: 243—258
- 22 Nowell G M, Kempton P D, Noble S R, et al. High precision Hf isotope measurements of MORB and OIB by thermal ionization mass spectrometry: insights into the depleted mantle. *Chem Geol*, 1998, 149: 211—233
- 23 Zheng Y F, Wu Y B, Zhao Z F, et al. Metamorphic effect on zircon Lu-Hf and U-Pb isotope systems in ultrahigh-pressure eclogite-facies meta-granite and metabasite. *Earth Planet Sci Lett*, 2005, 240: 378—400
- 24 Zheng Y F, Zhao Z F, Wu Y B, et al. Zircon U-Pb age, Hf and O isotope constraints on protolith origin of ultrahigh-pressure eclogite and gneiss in the Dabie orogen. *Chem Geol*, 2006, 231: 135—158
- 25 Zhang S B, Zheng Y F, Wu Y B, et al. Zircon U-Pb age and Hf-O isotope evidence for Paleoproterozoic metamorphic event in South China. *Precambrian Res*, 2006, 151: 265—288
- 26 McLennan S M, Hemming S R, Taylor S R, et al. Early Proterozoic crustal evolution: Geochemical and Nd-Pb isotopic evidence from metasedimentary rocks, southwestern North America. *Geochim Cosmochim Acta*, 1995, 59(6): 1153—1177
- 27 Wu R X, Zheng Y F, Wu Y B, et al. Reworking of juvenile crust: element and isotope evidence from Neoproterozoic granodiorite in South China. *Precambrian Res*, 2006, 146: 179—212
- 28 Xia X P, Sun M, Zhao G C, et al. LA-ICP-MS U-Pb geochronology of detrital zircons from the Jining Complex, North China Craton and its tectonic significance. *Precambrian Res*, 2006, 144: 199—212
- 29 Xia X P, Sun M, Zhao G C, et al. U-Pb and Hf isotopic study of detrital zircons from the Wulashan khondalites: Constraints on the evolution of the Ordos Terrane, Western Block of the North China Craton. *Earth Planet Sci Lett*, 2006, 241: 581—593
- 30 Darby B J, Gehrels G. Detrital zircon reference for the North China block. *J Asian Earth Sci*, 2006, 26(6): 637—648
- 31 Zhong C T, Deng J F, Wan Y S, et al. SHRIMP U-Pb Zircon dating of Adakite-sanukite-Closepet in the Daqingshan Area, Inner Mongol and its tectonic signification (in Chinese). In: Beijing SHRIMP Centre Annals (in Chinese). Beijing: Geological Publishing House, 2005. 27—29
- 32 Zhong C T, Deng J F, Wan Y S, et al. Magmatic records of Paleo-proterozoic Orogen in the northern margin of the North China Craton: Geochemical study and SHRIMP U-Pb zircon dating of strong peraluminous granitoids. In: Beijing SHRIMP Centre Annals (in Chinese). Beijing: Geological Publishing House, 2005. 30—31
- 33 Li J H, Yang C H, Du L L. SHRIMP U-Pb Geochronology evidence for the formation time of the Wanzi Group at Pingshan County, Hebei Province. *Prog Nat Sci* (in Chinese), 2004, 14(7): 774—781